Characterization of degradation products of Macitentan under various stress conditions by using Liquid Chromatography Mass Spectrometry

Naga Veera Yerra [a, c], Pavankumar Pallerla [a, c], Sukanya Pandeti [a,b,c], Jean-Claude Tabet [d], and Jagadeshwar Reddy Thota *[a,c]

[a]*Analytical Chemistry and Mass Spectrometry, CSIR-Indian Institute of Chemical Technology, Hyderabad-500 007, India.*

[b]*Medicinal and Process Chemistry Division, CSIR-Central Drug Research Institute, Lucknow- 226 031, India.*

[c]*Academy of Scientific and Innovative Research, New Delhi-110001, India.*

[d]*UPMC/IPCM (Chimie Biologique Organique et Structurale), UMR 7201, 4 place Jussieu, 75252 Paris Cedex 05, France.*

*Corresponding author

Dr. Jagadeshwar Reddy Thota

Analytical Chemistry and Mass Spectrometry

CSIR-Indian Institute of Chemical Technology

Hyderabad- 500 007, India

E-mail: tjreddy@iict.res.in

Tel: +91-(0) 2719 1767

Accepted Article

This article has been accepted for publication and undergone full peer review but has not been through the copyediting, typesetting, pagination and proofreading process which may lead to differences between this version and the Version of Record. Please cite this article as doi: 10.1002/rcm.8138

This article is protected by copyright. All rights reserved.

Abstract

Rationale

Stress testing of a drug candidate is an important step in drug discovery and development process. The presence of degradation products in a drug affects the quality as well as safety and efficacy of drug formulation. Hence, it is essential to develop an efficient analytical method which could be useful for the separation, identification and characterization of all possible degradation products of drug. Macitentan (MT) is an endothelin receptor antagonist (ERA) drug used to treat high blood pressure in the lungs. Comprehensive stress testing of MT drug was carried out as per ICH guidelines to understand the degradation profile of the drug.

Methods

MT was subjected to various stress conditions such as acidic, basic, neutral hydrolysis, oxidation, photolysis and thermal conditions; and the resulting degradation products were investigated using LC-DAD-ESI-HRMS and MS/MS techniques. An efficient and simple ultra-high performance liquid chromatography (UHPLC) method has been developed on Accucore C18 (4.6×150mm, 2.6µm) column using gradient elution of 5 mM ammonium formate and acetonitrile as mobile phases.

Results

The MT was found to degrade under acid and base hydrolysis stress conditions; whereas it was stable under oxidation, neutral hydrolysis, thermal and photolytic conditions. The MT formed nine DPs (DP1 to DP9) and one DP (DP10) under acidic and basic hydrolytic conditions, respectively. All the degradation products (DP1 to DP10) were identified and characterized by LC-MS/MS in positive ion mode with accurate mass measurements.

Conclusions

MT was found to be labile under hydrolytic conditions. The structures of the degradation products were characterized by appropriate mechanisms. The proposed method can be effectively used for the characterization of MT and its degradation products.

Keywords

Macitentan, Stress conditions, LC-DAD-ESI/MS/MS, Accurate mass measurements and Degradation products.

Accepted Article

This article is protected by copyright. All rights reserved.

Introduction

Macitentan is an endothelin receptor antagonist (ETA) that has been widely used in the therapy of pulmonary arterial hypertension (PlAHT).[1-3] The endothelin (ET) is a twenty one amino acid peptide that was generated from a thirty nine amino acid precursor and is one of the most effective and long lasting vasoconstrictor.[2,3] There are three isoforms of the endothelin: endothelin-1 (ET-1), endothelin-2 (ET-2) and endothelin-3 (ET-3). ETs regulate different biologic processes such as tissue remodelling, tissue repair, cellular differentiation, smooth muscle cell proliferation and inflammation.[3-5]

PlAHT is a serious disease affecting fifteen individuals per million annually.[6] It is characterized by sustained elevation of pulmonary vascular resistance, which finally leading to right heart failure and premature death. Clinically, PlAHT patients present with nonspecific symptoms of decreased exercise tolerance and shortness of breath on exertion. According to group diagnosis of PlAHT World Health Organization (WHO) is confirmed by a mean pulmonary arterial pressure ≥25 mmHg with pulmonary artery wedge pressure ≤15 mmHg wood units, as measured by cardiac catheterization.[7-9] The drug Macitentan {N-[5-(4-bromophenyl)-6-[2-[(5-bromo-2 pyrimidinyl)oxy]ethoxy]-4-pyrimidinyl]-N'-propylsulfamide}, which is the modified structure of bosentan with the aim of improving its medicinal activity.[10-11]

Stress testing of a drug aspirant is a decisive constituent of both drug discovery, drug development and the regulatory approval perspective.[12] International Conference on Harmonization (ICH) and other international agencies suggested that all degradation products formed during the forced degradation of a drug under various stress conditions should be characterized.[13,14] Further, structure elucidation of degradation products and unknown impurities is also required to help chemists modify their novel compounds to prepare drug candidates with improved stability and determine whether impurities and degradation products have any toxicity.[15-18]

In addition, stress testing can help in the selection of more stable drug substance salt forms and drug formulations.[19] It is well accepted that the drug degradation in formulations is highly complex and often unpredictable process. The degradation products usually arise from the ingredients used in dosage formulation and/or in the process of formulation where temperature, humidity and light play a part. The degradation products can be generated from hydrolysis, oxidation, adduct formation, dimerization, rearrangement and often the combination of these processes. If toxic degradation products were formed under optimum

This article is protected by copyright. All rights reserved.

Accepted Article

natural conditions which lead to allergic reactions and have fatal consequences.[20] To accelerate drug development, various stress-testing protocols were designed to emulate the stresses that the compound may experience during manufacturing and storage conditions. Hence, the goal of the present study is to conduct the forced degradation study on Macitentan as per the ICH prescribed conditions to identify the possible degradation products arising under various stress conditions like hydrolysis, photolysis and oxidation. Estimation of Macitentan and its metabolites in biological matrices and in formulations have been reported in the literature.[21] However, to the best of our knowledge, no attempts have been made for the identification of degradation products of Macitentan according to ICH guidelines. Mass spectrometry (MS) coupled with liquid chromatography technique has been widely used in the analysis of drug degradation products.[22,23] High resolution mass measurements in mass spectra and product ion spectra enable identification and structure elucidation of drug degradation products. High resolution mass measurements can be achieved by mass analyzers such as time-of-flight (ToF), Fourier transform orbital trap (FTMS-Orbitrap) and Fourier transform ion cyclotron resonance (FTICR) mass spectrometers.[24,25] Hence, we have undertaken the present study to characterize Macitentan and all its degradation products using ultra high performance liquid chromatography (UHPLC) coupled with Qq-TOF tandem mass spectrometer.

Experimental

Drugs and reagents

MT was isolated from the capsules purchased from the local market. The material grinded and then further subjected to flash chromatography on a column of C18 (15-25µM particle size, 100 Aº pore size procured from Fluka, Bangalore, India) and eluted with water - acetonitrile (20:80) to afford Macitentan (MT). The compound's visualization was done under UV light and by spraying with 10% sulphuric acid in methanol. The structure of the compound was confirmed by spectroscopic techniques such as NMR, FTIR and UV (Figure S1 to Figure S4, Supporting Information); the purity of the isolated MT was found to be >98.9 %. LC-MS grade acetonitrile (ACN) was purchased from Sigma-Aldrich (Bangalore, India). Analytical reagent (AR) grade ammonium formate, hydrochloric acid (HCl) and sodium hydroxide (NaOH) were purchased from S.D. Fine Chemicals (Mumbai, India). Analytical reagent grade Hydrogen peroxide 30% was purchased from Merck (Mumbai, India). Deionized water (18 MΩ) was obtained from a Milli-Q apparatus (Millipore, Bedford, MA, USA).

This article is protected by copyright. All rights reserved.

Instrumentation

Chromatographic separations of MT and its degraded samples were achieved on Surveyor UHPLC system (Agilent Technologies, Germany) consisting a quaternary gradient pump, an auto-injector and an in-line degasser. The column compartment with a 23 ºC temperature and a Diode Array Detector (DAD) was employed throughout the analysis.

Mass spectral analysis was carried out on Agilent Technologies mass spectrometer (6545 Q-TOF LC/MS, Germany). The eluent of UHPLC was directed into mass spectrometer through electrospray ionization (ESI) interface and operated in the positive ionization mode. The mass spectrometer was calibrated before analysis using the manufacturer's calibration solution.-Parameters of the ion source were as follows: Gas temperature 280 °C, Gas flow 8 L/min, Nebulizer 30 psig, Sheath gas temperature 300 °C, Sheath gas flow 11.8 L/min, V_{Cap} 3200 V, Nozzle voltage 1000 V, Fragmentor 80 V, Skimmer 1 60 V. Nitrogen was used as the sheath gas. The mass spectra were recorded over a *m/z* range of 50 *m/z* -1700 *m/z*. MS/MS experiments were carried out by collision induced dissociation (CID) mode at E_{Lab}=30 eV , which is the optimal collision energy for the best fragmentation, and ultra pure N_2 gas was used as collision gas. DAD, MS and MS/MS data were processed using Mass Hunter Workstation Software (v B.07.00)

An ultra-sonicator from Power Sonic-405 (Hwashin Technology Co. Seoul, South Korea), weighing was carried out on a Mettler Toledo (ML204, Switzerland) and pH meter from pH tutor (Eutech Instruments, Singapore) were used to dissolve the sample and measure the pH of the mobile phase, respectively. The hydrolytic and thermal stress degradation studies were carried out using a high precision water bath and hot air oven equipped with digital temperature controller to maintain the temperature within the range of ±2 ºC and ±1 ºC, respectively (Osworld scientific Pvt. Ltd. India).

Photo degradation was carried out in a photo stability chamber (Osworld OPSH-G-16-GMP series, Osworld scientific Pvt. Ltd. India) capable of controlling the temperature and humidity within a range of 40 ± 5 °C/75% ±3 % RH (relative humidity).[26]

Optimization of the chromatographic conditions

The chromatographic separation method was developed on Accucore C18 (4.6×150mm, 2.6 µm) (Thermo Scientific, North America) column. The method was optimized by varying the selectivity determination factors such as pH of mobile phase, ratio of organic solvent, flow rate. During scouting experiments, it was found that a few hydrolysis degradation products were not resolved in formic acid and ammonium acetate buffers with

This article is protected by copyright. All rights reserved.

different pH. Finally, acceptable separation was achieved using 5 mM ammonium formate in water (A) buffer and acetonitrile (B) as organic modifier with a flow rate of 0.3 mL min^{-1} in gradient elution mode. The following linear gradient elution was used: (time in min/proportion of solvent B): 0–2/20, 2–25/80, 25-30/80, 30-38/20, and 38-40/20. Column was equilibrated with 20 column volumes of mobile phase at the initial gradient composition prior to sample injection. The injection volume was 1µl and all the stress samples were analysed using a DAD (200–400 nm) detector. Absorption chromatograms were extracted at 250 nm to detect the peaks of all the degradation products.

Stress degradation studies

Stress studies were carried out on 1 mg/ml solution of MT as per ICH recommended conditions of hydrolysis, oxidation, thermal and photolysis. As the drug was sparingly soluble in water and freely soluble in acetonitrile, all the stress samples were prepared in H_2O/ ACN (1:1 v/v). Hydrolytic stress degradation study was carried out in 1N HCl, 1N NaOH and water at 80 ºC for 4 h, 6 h and 48 h, respectively. For oxidative stress degradation, MT was subjected to 30 % H_2O_2 at room temperature for 24 h. Based on "A stress testing benchmarking study" pharmaceutical companies typically carry out the thermal degradation studies at ≥70 ºC temperature. Hence in the present study, thermal degradation was carried out in solid state by exposing pure MT in a Petri plate with a very thin layer to dry heat at 80 ºC for 5 days.

A photolytic stress study was carried out in solid form at 40 ºC in a photo stability chamber, equipped with white fluorescent light source designed for emitting significant radiation at 320 nm and a near UV fluorescent lamp with energy emission between 350 and 370 nm for providing an overall illumination of not less than 1.2 million lux hours and irradiation density of not less than 200 W m^{-2}. The distance of Petri dish from light source is about 10 cm. The optimized stress conditions of MT was given in supplementary Table S1 (supporting information).

Sample preparation

All the stressed sample (hydrolytic, oxidative, thermal and photolytic) solutions were stored in dark at the same temperature to serve as control (MT). Samples were prepared by filtering the solution through 0.22 µm filter unit prior to UHPLC-DAD-ESI-HRMS analysis. Samples were withdrawn at different time interval and diluted with mobile phase before injection. Both the acid and base degradation samples were neutralized with 1N NaOH and

This article is protected by copyright. All rights reserved.

1N HCl, respectively, prior to analysis. The final concentrations of 50 ppm of the samples were prepared in acetonitrile/water (1:1 v/v) before injecting into UHPLC-DAD-ESI-HRMS.

Results and discussion

The degradation behaviour of MT was studied by using UHPLC-DAD-ESI-HRMS under various forced degradation conditions. The drug found to be degraded under hydrolytic conditions (acidic and basic), while it was found to be stable in oxidative, photolytic, thermal and neutral hydrolytic conditions. The degradation of MT under acidic (1N HCl at 80 °C for 4 hrs) conditions yielded nine degradation products (DP1 to DP9) whereas under basic (1N NaOH at 80 °C for 6 hrs) hydrolytic conditions the drug resulted in one degradation product (DP10). The UHPLC-DAD chromatograms and extracted ion chromatograms (EICs) of MT and its stress degradation samples are shown in supplementary Figure S5 and Figure S6 (Supporting information), respectively.

LC-mass spectrum and product ion spectrum studies of MT and its degradation products

MT and all its degradation products DP1-DP10 showed abundant $[M+H]^+$ ions in their ESI-HR mass spectra. Suitable elemental compositions were derived from the accurate mass measurement of $[M+H]^+$ ions of MT and its DPs. The proposed structures of all the DPs and their mass spectral data (MS/MS) with elemental compositions are given in Figure 1 and Table 1, respectively. With a view to elucidate the structure of DPs, the $[M+H]^+$ ion of MT at *m/z* 586.9705 ($C_{19}H_{21}Br_2N_6O_4S$, Rt = 27.48 min) was subjected to MS/MS analysis. The product ion spectrum thus obtained is shown in Figure S7 (i). The product ion spectrum showed low abundant ions at *m/z* 466 and *m/z* 413 in the high-*m/z* ratio region that were formed by the loss of $C_3H_7NSO_2$ and $C_4H_3N_2OBr$ moieties from the $[M+H]^+$ ion, respectively (Scheme 1). The $[M+H]^+$ ion coexist in different forms which allow different fragmentation pathways. The ion at *m/z* 466 underwent loss of $C_{10}H_8N_3OBr$ by the bond cleavage between 'O' and 'C' resulted in the highly resonance stabilised structure indicative fragment ion at *m/z* 201 (the base peak). The product ion spectrum dominated by the formation of ion at *m/z* 201 which is a favourable process whereas the other ions are of low abundance. The ion at *m/z* 201 further produced a distonic ion (at *m/z* 122) by the loss of more stable $Br^{\cdot}$ radical.[27,28] The product ion spectrum of MT also showed low abundant fragment ions at *m/z* 292 and *m/z* 175 that were formed from the $[M+H]^+$ ion through proton transfer reaction intermediates

This article is protected by copyright. All rights reserved.

(ion-neutral complexes) as depicted in Scheme 1. The elemental compositions of all the product ions were confirmed by the accurate mass measurements (Table 1).

The DP1 showed $[M+H]^+$ ion at *m/z* 174.9402 ($C_4H_4N_2BrO$, Rt = 4.66 min) in its ESI-HR mass spectrum. This was lower by 412 Da when compared to that of $[M+H]^+$ ion of MT, which indicated that the DP1 could be formed by the elimination of $C_{15}H_{17}BrN_4O_3S$ from the MT (Scheme 2) under acidic hydrolytic conditions. As per nitrogen rule the DP1 containing even number of nitrogen atoms and the obtained natural isotopic ratio (1:1) suggested presence of one bromine atom. The product ion spectrum of DP1 at *m/z* 175 showed characteristic odd-electron product ions at *m/z* 96, *m/z* 68 and *m/z* 41 that were formed by involving stable $Br^{\cdot}$ radical loss as depicted in Scheme S1, supporting information. The other product ions at *m/z* 157, *m/z* 148 and *m/z* 147 were formed by the loss of H_2O, HCN, and CO, from the $[M+H]^+$ ion, respectively (see Figure S7 (ii), Scheme S1, supporting information). The less abundant ions at *m/z* 148 and *m/z* 147 further yielded ions at *m/z* 105 and *m/z* 120 by the loss of CHNO and HCN moieties, respectively. All these data (Table 1) were highly compatible with the proposed DP1 structure as 5-bromopyrimidin-2-ol.

The ESI-HR mass spectrum of DP2 showed $[M+H]^+$ ion at *m/z* 236.9413 (Rt = 9.55 min) with an elemental composition of $C_6H_7BrClN_2O$. It suggested that the DP2 could be formed due to the nucleophilic substitution on the oxygen linked carbon with chloride ion (Scheme 2,). The $[M+H]^+$ ion (*m/z* 237) of the DP2 displayed isotopic ratio of 3:4:1 that suggested the presence of one bromine and one chlorine atoms. The product ion spectrum of DP2 showed the complementary product ions at *m/z* 175 and *m/z* 63 that were generated by the loss of C_2H_3Cl and $C_4H_3N_2OBr$ moieties *via* formation of ion-neutral complex prior to dissociation from the $[M+H]^+$ ion, respectively (see Figure S7(iii), supporting information). Ion-neutral complexes which often yield complementary product ions with a sum of *m/z* equal to that of precursor ion with a shift of +1 *m/z* in the positive mode. In addition, the observed structure indicative product ions at *m/z* 157, *m/z* 147 and *m/z* 120 were found to be similar to DP1 (see Scheme S2, supporting information). On the basis of characteristic fragment ions and proposed fragmentation pattern with accurate mass data (Table 1), the DP2 was identified as 5-bromo-2-(2-chloroethoxy) pyrimidine.

The DP3 showed $[M+H]^+$ ion at *m/z* 265.9930 (Rt = 11.12 min, $C_{10}H_9BrN_3O$) in its ESI-MS mass spectrum. The isotopic pattern of the $[M+H]^+$ ion (ratio of 1:1) and the nitrogen rule suggested the presence of one bromine atom and odd number of nitrogen atoms. The product ion spectrum of DP3 (see Figure S7 (vi), supporting information) showed primary

This article is protected by copyright. All rights reserved.

losses of HCN and Br· radical from the $[M+H]^+$ ion resulted in the ions at *m/z* 239 and *m/z* 187, respectively. Further, the fragment ions at *m/z* 239 and *m/z* 187 produced ions at *m/z* 222 and *m/z* 160 by the loss of NH_3 and HCN, respectively, as described in Scheme S3 (supporting information). Based on the proposed fragmentation with accurate mass data (Table 1) the DP3 was characterized as 6-amino-5-(4-bromophenyl) pyrimidin-4-ol. A probable mechanism for the formation of DP3 is illustrated in Scheme 2.

The DP4 was eluted at Rt = 13.23 min and the ESI-HRMS spectrum showed $[M+H]^+$ ion at *m/z* 292.0077 with an elemental composition of $C_{12}H_{11}BrN_3O$. Based on the obtained isotopic distribution of $[M+H]^+$ ion and nitrogen rule the DP4 might contain one bromine atom and odd number of nitrogen atoms. This could be formed due to stepwise elimination of $C_3H_7NSO_2$ and $C_4H_3ON_2Br$ groups from the MT as shown in Scheme 2. In the MS/MS analysis (see Figure S7 (v), supporting information), the product ions at *m/z* 265 and *m/z* 213 (odd-electron ion) were formed by the loss of HCN and Br· radical, respectively, from the $[M+H]^+$ ion. The fragment ion at *m/z* 186 was yielded by the expulsion of HCN group from the ion at *m/z* 213. Further, the product ions at *m/z* 239 and *m/z* 222 were yielded by the sequential elimination of C_2H_2 and NH_3 moieties from the ion at *m/z* 265. On the basis of characteristic fragment ions and proposed fragmentation pattern with accurate mass data (see Scheme S4, supporting information and Table 1), the DP4 was identified as 5-(4-bromophenyl)-6-(vinyloxy) pyrimidin-4-amine.

DP5 (Rt = 14.94 min) was formed as a minor degradation product under acidic stress conditions, and its ESI-HRMS spectrum showed an $[M+H]^+$ ion at *m/z* 310.0182 ($C_{12}H_{13}BrN_3O_2$), which was lower by 277 Da when compared to the MT. This could be formed by the elimination of $C_3H_7NSO_2$ and 5-bromopyrimidine groups from the MT during acidic hydrolysis conditions as depicted in Scheme 2. The product ion spectrum showed fragment ions at *m/z* 292 and *m/z* 266 that were formed by the loss of H_2O and C_2H_4O moieties, respectively, from the ion at *m/z* 310 (see Figure S7(vi) and Scheme S5, supporting information). The ion at *m/z* 266 was formed through ion-neutral complex formation. The other characteristic ions at *m/z* 239 and *m/z* 222 were formed by the sequential expulsions of HCN and NH_3 molecules, respectively, from the ion at *m/z* 266 through ring opening process as shown in Scheme S5 (supporting information). Based on all these data (Table 1), DP5 was characterized as 2-((6-amino-5-(4-bromophenyl) pyrimidin-4-yl)oxy)ethan-1-ol.

Accepted Article

This article is protected by copyright. All rights reserved.

The DP6 was eluted at Rt = 15.74 min and the ESI-HRMS spectrum showed $[M+H]^+$ ion at *m/z* 387.0137 with an elemental composition of $C_{13}H_{16}BrN_4O_3S$ (Table 1). Based on the mass difference between DP6 and MT (200 Da) and obtained elemental composition, it was assumed that the DP6 was formed by the loss of 5-bromo-2-(vinyloxy)pyrimidine from MT during the acid hydrolysis, as shown in Scheme 2. The product ion spectrum of the $[M+H]^+$ ion of DP6 showed complementary fragment ions at *m/z* 328 and *m/z* 60 that were yielded by the loss of C_3H_9N and $C_{10}H_6N_3O_3SBr$ moieties *via* formation of ion-neutral complex prior to dissociation from the $[M+H]^+$ ion, respectively (Scheme S6, supporting information). The formation of other characteristic odd-electron fragment ions at, *m/z* 249 and *m/z* 185 were formed by the sequential elimination of $Br^{\cdot}$ radical and SO_2 from the ion at *m/z* 328 (see Figure S5(vii), supporting information) as described in Scheme S6, supporting information. The other fragment ion at *m/z* 266 was found to be similar to that of obtained in DP5. All these data were in good agreement with the proposed DP6 structure as N-[5-(4-Bromophenyl)-6-hydroxy-4-pyrimidinyl]-N’-propylsulfamide.

The ESI-HRMS spectrum displayed an $[M+H]^+$ ion at *m/z* 327.9851 (Rt = 16.97 min, $C_{12}H_{12}BrClN_3O$) (Table 1) for DP7. This compound could be formed due to the nucleophilic substitution on DP5 with Cl^- anion to yield DP7, as depicted in Scheme 2. The isotopic distribution of $[M+H]^+$ ion (3:4:1) indicated the presence of one bromine and one chlorine atoms. The product ion spectrum of DP7 showed ion at *m/z* 292 that was produced by the loss of HCl moiety from the $[M+H]^+$ ion (see Figure S7(viii), Scheme S7, supporting information). The formation of product ions at *m/z* 266 and 239 were similar to that of DP5. The other odd-electron fragment ion at *m/z* 249 and *m/z* 187 were yielded by the sequential loss of $Br^{\cdot}$ radical and C_2H_3Cl group from the $[M+H]^+$ ion. Based on these data the DP7 was characterised as 5-(4-bromophenyl)-6-(2-chloroethoxy) pyrimidin-4-amine.

The acidic degradation product DP8 was eluted at Rt = 21.92 min and its ESI-HRMS showed $[M+H]^+$ ion at *m/z* 449.0050 ($C_{15}H_{19}BrClN_4O_3S$). The $[M+H]^+$ ion of DP8 was shifted by -138 Da when compared to the $[M+H]^+$ ion of MT, which suggested that 5-bromopyrimidin-2-ol was eliminated from MT to form DP8 as depicted in Scheme 2. The isotopic ratio of $[M+H]^+$ suggested the presence of one bromine and one chlorine atoms. The product ion spectrum of DP8 showed product ions at *m/z* 390, *m/z* 328 and *m/z* 60 that were generated by the loss of C_3H_9N, $C_3H_7NSO_2$ and $C_{12}H_9BrClN_3O_3$ moieties through the formation of ion-neutral complex prior to dissociation from the $[M+H]^+$ ion, respectively (Scheme 3) (see Figure S7 (ix), supporting information). The observed complementary

This article is protected by copyright. All rights reserved.

product ions at *m/z* 390 and *m/z* 60 provided structural information of DP8. The product ions at *m/z* 328 and *m/z* 292 were similar to that of DP7. In addition, an odd-electron product ion at *m/z* 311 was formed by the loss of $Br^{\cdot}$ radical, from the product ion at *m/z* 390 as depicted in Scheme 3. Based on the proposed fragmentation pattern, supported by the elemental compositions, (Table 1) DP8 was characterized as N-[5-(4-Bromophenyl)-6-[2-chloroethoxy]-4-pyrimidinyl]-N'-propylsulfamide.

The ESI-HR mass spectrum of acidic degradation product DP9 showed $[M+H]^+$ ion at *m/z* 465.9516 (Rt = 23.82 min) with an elemental composition of $C_{16}H_{14}Br_2N_5O_2$ (Table 1). DP9 could be formed due to the elimination of $C_3H_7NSO_2$ moiety from the MT (Scheme 2). The natural isotopic pattern of $[M+H]^+$ ion (1:2:1) suggested the presence of two bromine atoms in DP9. The product ion spectrum of the $[M+H]^+$ ion showed structure indicative product ions at *m/z* 292 and *m/z* 175 by the loss of $C_4H_3BrN_2O$ and $C_{12}H_{10}BrN_3O$ groups *via* ion-neutral complex prior to dissociation from the ion at *m/z* 466, respectively (see Figure S7(x), supporting information). Further, the ion at *m/z* 175 showed loss of H_2O resulting in the ion at *m/z* 157 which was similar to that of DP1 (see Scheme S8, supporting information). Based on all these data, DP9 was characterized as 5-(4-bromophenyl)-6-(2-((5-bromopyrimidin-2-yl)oxy)ethoxy)pyrimidin-4-amine.

The alkaline hydrolyzed compound, DP10 showed $[M+H]^+$ ion at *m/z* 431.0380 ($C_{15}H_{20}O_4N_4SBr$, Rt = 19.98 min). This $[M+H]^+$ ion was lighter by 156 Da than that of the MT (*m/z* 587). This product could be formed by the elimination of 5-bromopyrimidine from the MT through C-O bond cleavage of MT to form alcohol under basic hydrolytic conditions as depicted in Scheme S9 (supporting information). Based on the isotopic distribution of $[M+H]^+$ ion and nitrogen rule the DP10 might contain one bromine atom and even number of nitrogen atoms. In the ESI-MS/MS analysis, the product ion spectrum of *m/z* 431 (see Figure S2(xi), supporting information) showed structure indicative complementary product ions at *m/z* 372 and *m/z* 60 that were formed by the loss of C_3H_9N and $C_{12}H_{10}BrN_3O_4S$ moieties, respectively, from the $[M+H]^+$ ion through ion-neutral complex. An odd-electron product ion at *m/z* 293 was produced by the loss of $Br^{\cdot}$ radical from the ion at *m/z* 372. In addition, the observed other characteristic fragment ion at *m/z* 387 formed by the loss C_2H_4O group from the $[M+H]^+$ ion, which is same as $[M+H]^+$ ion of DP6 and all the product ions of DP6 were also observed for DP10 (Scheme 4). On the basis of above data (Table 1) the DP10 was

This article is protected by copyright. All rights reserved.

characterized as N-[5-(4-Bromophenyl)-6-[2-hydroxyethoxy]-4-pyrimidinyl]-N-propyl sulfamide.

Conclusions

In this report, the degradation of MT under various stress conditions was carried out as per the ICH guidelines. The drug was found to be labile under acidic and basic hydrolytic conditions, whereas it was found to be stable in thermal, photolytic and neutral hydrolytic conditions. In the acidic hydrolytic condition the MT formed nine DPs (DP1 to DP9) whereas in the basic hydrolytic conditions the MT formed only one DP (DP10). All these DPs were characterized by LC-DAD-ESI-HRMS and MS/MS analysis. A complete degradation pathway of the drug was established in various stress conditions. The proposed method can be effectively used to carry out structural characterization of MT and its degradation products.

Acknowledgments

The authors thank the Director, IICT, Hyderabad, for facilities. The authors also thankful to Ms. Shirisha B for her help. N.V.Y, P.K.P and S.P. are grateful to CSIR, New Delhi, for the award of Research Fellowships.

References

1. Bruderer S, Hopfgartner G, Seiberling M, Wank J, Sidharta PN, Treiber A, Dingemanse J. Absorption, distribution, metabolism, and excretion of macitentan, a dual endothelin receptor antagonist, in humans. *Xenobiotica*. 2012;42:901‐10.
2. Lepist EI, Gillies H, Smith W, Hao J, Hubert C, St Claire RL , Brouwer KR, Ray AS. Evaluation of the endothelin receptor antagonists ambrisentan, bosentan, macitentan, and sitaxsentan as hepatobiliary transporter inhibitors and substrates in sandwich-cultured human hepatocytes. *PLoS One*. 2014;9:e87548.
3. Iglarz M, Binkert C, Morrison K, Fischli W, Gatfield J, Treiber A, Weller T, Bolli MH, Boss C, Buchmann S, Capeleto B, Hess P, Qiu C, Clozel M. Pharmacology of macitentan, an orally active tissue‐targeting dual endothelin receptor antagonist. *J Pharmacol Exp Ther*. 2008;327:736‐45.
4. Sitbon O, Morrell N. Pathways in pulmonary arterial hypertension: The future is here. *Eur Respir Rev*. 2012;21:321‐7.
5. Seferian A, Simonneau G. Therapies for pulmonary arterial hypertension where are we today, where do we go tomorrow. *Eur Respir Rev*. 2013;22:217‐26

This article is protected by copyright. All rights reserved.

Accepted Article

6. Badesch DB, Raskob GE, Elliott CG, Krichman AM, Farber HW, Frost AE, Barst RJ, Benza RL, Liou TG, Turner M, Giles S, Feldkircher K, Miller DP, McGoon MD. Pulmonary Artery Hypertension: baseline Characteristics From the REVEAL registry. *Chest*. 2010;137(2):376-87.
7. Marius MH, Harm JB, Robin C, Robert F, Dinesh K, Marcin K, David L, Alessandra M, Toru S, Fernando T, Martin RW, David BB. Definitions and diagnosis of pulmonary hypertension. *J. Am. Coll. Cardiol*. 2013;62(25):D42-D50.
8. Badesch DB, Abman SH, Simonneau G, Rubin LJ, McLaughlin VV. Medical therapy for pulmonary arterial hypertension: updated ACCP evidence-based clinical practice guidelines. *Chest.* 2007;131:1917-1928.
9. ADEMPAS R _ (riociguat) tablets for oral use. Full prescribing information. 2014. Whippany, NJ: Bayer HeathCare Pharmaceuticals, Inc. https://www.accessdata.fda.gov/drugsatfda_docs/label/2017/204819s006lbl.pdf.
10. Iglarz M, Binkert C, Morrison K, Fischli W, Gatfield J, Treiber A, Weller T, Bolli MH, Boss C, Buchmann S, Capeleto B, Hess P, Qiu C, Clozel M. Pharmacology of macitentan, an orally active tissue-targeting dual endothelin receptor antagonist. *J. Pharmacol. Exp. Ther*. 2008;327:736-745.
11. John G , Celia MG, Thomas S, Martine C, Oliver N. 2012. Slow receptor dissociation kinetics differentiate macitentan from other endothelin receptor antagonists in pulmonary arterial smooth muscle cells. *PLoS One*. 2012;7: e47662.
12. CPMP. Note for Guidance on Stability Testing: Stability Testing of Existing Active Substances and Related Finished Products. Committee for Proprietary Medicinal Products, EMEA, London, 2002. http://www.ema.europa.eu/docs/en_GB/document_library/Scientific_guideline/2009/09/WC500003466.pdf.
13. ICH. Stability testing of new drug substances and products Q1A (R2). International Conference on Harmonization, IFPMA, Geneva, 2003. https://www.ich.org/fileadmin/Public_Web_Site/ICH_Products/Guidelines/Quality/Q1A_R2/Step4/Q1A_R2__Guideline.pdf.
14. WHO. Stability Testing of Active Pharmaceutical Ingredients and Pharmaceutical Products. World Health Organization: Geneva, 2007. http://apps.who.int/medicinedocs/documents/s19133en/s19133en.pdf.
15. Borkar. R. M, Raju.B, Devrukhakar. P. S, Tondepu. N, Rao. A. B. N, R. Srinivas. Liquid chromatography/electrospray ionization tandem mass spectrometric study of

This article is protected by copyright. All rights reserved.

Accepted Article

milnacipran and its stressed degradation products. *Rapid Commun. Mass Spectrum*. 2013;*27*:369.

16. Borkar RM, Raju B, Srinivas R, Patel P, Shetty SK. Identification and characterization of stressed degradation products of metoprolol using LC/Q-TOF-ESI-MS/MS and MS^n experiments. *Biomed. Chromatogr*. 2012;*26*:720.
17. Purna Chander C, Raju B, Sulthana A, Srinivas R. LC-ESI-MS/MS study of carvedilol and its stress degradation products. *Anal. Methods*. 2013;*5*:4330.
18. Raju B, Ramesh M, Srinivas R, Raju SS, Venkateswarlu Y. Identification and characterization of stressed degradation products of prulifloxacin using LC-ESI-MS/Q-TOF, MS^n experiments: Development of a validated specific stability-indicating LC-MS method. *J. Pharm. Biomed. Anal.* 2011;*56*:560.
19. Prinesh Patel N, Roshan Borkar M, Pradipbhai Kalariya D, Rahul Gangwal P, Abhay Sangamwar T, Gananadhamu S, Srinivas R. Characterization of degradation products of Ivabradine by LC-HR-MS/MS: a typical case of exhibition of different degradation behavior in HCl and H_2SO_4 acid hydrolysis. *J. Mass Spectrom*. 2015;*50*:344-353.
20. McMahon W, Pratt RG, Hammad TA, Kozlowski S, Zhou E, Lu S, Kulick CG, Mallick T, Dal Pan G. Description of hypersensitivity adverse events following administration of heparin that were potentially contaminated with over sulfated chondroitin sulfate in early 2008. *Pharmacoepidemiol. Drug Safety*. 2010,*19*;921.
21. Sanjay M, Bhagavatula K, Srinivasa S, Rogério S, Adam T, Hossein-Ardeschir G, Richard NC, Marion D, Tomás P, Gérald S, John W, Lewis JR, Pavel J, Elke H, Galiè N, Loïc P, Olivier S. Macitentan improves health-related quality of life in pulmonary arterial hypertension: results from the randomized controlled SERAPHIN trial. *Am. J. Respir. Crit. Care Med.* 2013;187:A3269.
22. Sukanya P, Tofan Kumar R, Narender T, Jagadeshwar Reddy T. Identification of stress degradation products of iloperidone using liquid chromatography coupled with an Orbitrap mass spectrometer. *Rapid Commun Mass Spectrom*. 2017;31:1324-1332.
23. Kalariya PD, Talluri MVNK., Ragampeta S. Experimental design approach for selective separation of vilazodone HCl and its degradants by LC-PDA and characterization of major degradants by LC/QTOF-MS/MS. *Chromatographia*. 2014;77:1299-1313.
24. Dietrich AV. Principles of high-resolution MS: Applications of High-Resolution Mass Spectrometry in Drug Discovery and Development. 2014**:**6-20. https://doi.org/10.4155/9781909453555.

This article is protected by copyright. All rights reserved.

Accepted Article

25. Junot C, Fenaille F, Colsch B, Bécher F. High Resolution Mass Spectrometry Based Techniques at the crossroads of Metabolic Pathways. *Mass Spectrom Rev*. 2014;33:471–500.
26. ICH guideline Q3C (R6) on impurities: guideline for residual solvents EMA/CHMP/ICH/82260/2006, CHMP, 2016. http://www.ema.europa.eu/docs/en_GB/document_library/Scientific_guideline/2011/03/WC500104258.pdf.
27. Wilfried MAN, Ricardo ACC. Fragmentation of even-electron ions: Interpretation of MS-MS Mass Spectra of Drugs and Pesticides. 2017: 91 (John Wiley & Sons, Inc.)
28. Jonathan PW, Nico MMN, Brian NG, Vibhuti JP, James HS. Collision-induced fragmentation pathways including odd-electron ion formation from desorption electrospray ionisation generated protonated and deprotonated drugs derived from tandem accurate mass spectrometry. *J. Mass Spectrom*. 2006;41:1277–1286.

Accepted Article

This article is protected by copyright. All rights reserved.

Table 1. Elemental composition of precursor and product ions of MT and its degradation products.

MT and its DPs (Retention time in min.)	*Elemental composition*	*Theoretical m/z*	*Experimental m/z*	*Mass error (Δ ppm)*
MT(27.48)	$C_{19}H_{21}Br_2N_6O_4S^+$	586.9706	586.9705	0.25
	$C_{16}H_{14}Br_2N_5O_2^+$	465.9509	465.9508	0.16
	$C_{15}H_{18}BrN_4O_3S^+$	413.0278	413.0279	-0.25
	$C_{12}H_{11}BrN_3O^+$	292.0080	292.0089	-3.14
	$C_6H_6BrN_2O^+$	200.9658	200.9659	-0.67
	$C_4H_4BrN_2O^+$	174.9502	174.9500	1
	$C_6H_6N_2O^{+\cdot}$	122.0475	122.0471	2.64
DP1(4.66)	$C_4H_4BrN_2O^+$	174.9502	174.9402	-0.03
	$C_4H_2BrN_2^+$	156.9396	156.9395	0.38
	$C_3H_3BrNO^+$	147.9393	147.9397	-2.75
	$C_3H_4BrN_2^+$	146.9552	146.9552	-0.15
	$C_3H_3BrN^+$	119.9443	119.9438	4.22
	$C_2H_2Br^+$	104.9334	104.9334	0.42
	$C_4H_4N_2O^{+\cdot}$	96.0318	96.0315	2.76
	$C_3H_4N_2^{+\cdot}$	68.0369	68.0367	3.85
	$C_2H_3N^{+\cdot}$	41.0260	41.0258	1.8
DP2(9.55)	$C_6H_7BrClN_2O^+$	236.9425	236.9413	4.9
	$C_4H_4BrN_2O^+$	174.9502	174.9498	1.79
	$C_4H_2BrN_2^+$	156.9396	156.9392	2.38
	$C_2H_3BrN^+$	119.9443	119.9422	1.53
	$C_2H_4Cl^+$	62.9996	62.9993	4.72
DP3(11.12)	$C_{10}H_9BrN_3O^+$	265.9924	265.9930	-2.27
	$C_9H_8BrN_2O^+$	238.9815	238.9819	-1.68
	$C_9H_5BrNO^+$	221.9549	221.9552	-1.45
	$C_{10}H_9N_3O^{+\cdot}$	187.0740	187.0746	-3.12
	$C_9H_8N_2O^{+\cdot}$	160.0631	160.0630	0.65
DP4(13.23)	$C_{12}H_{11}BrN_3O^+$	292.0080	292.0077	-1.15
	$C_{11}H_{10}BrN_2O^+$	264.9971	264.9974	-1.18
	$C_9H_8BrN_2O^+$	238.9815	238.9807	3.03
	$C_9H_5BrNO^+$	221.9549	221.9544	2.39
	$C_{12}H_{11}N_3O^{+\cdot}$	213.0897	213.0895	0.9
	$C_{11}H_{10}N_2O^{+\cdot}$	186.0788	186.0786	0.94

Accepted Article

This article is protected by copyright. All rights reserved.

DP5(14.94)	$C_{12}H_{13}BrN_3O_2^+$	310.0186	310.0182	1.13
	$C_{12}H_{11}BrN_3O^+$	292.0080	292.0074	1.91
	$C_{10}H_9BrN_3O^+$	265.9924	265.9922	0.45
	$C_9H_8BrN_2O^+$	238.9815	238.9821	-2.7
	$C_9H_5BrNO^+$	221.9549	221.9544	2.31
DP6(15.74)	$C_{13}H_{16}BrN_4O_3S^+$	387.0121	387.0137	-4.24
	$C_{10}H_7BrN_3O_3S^+$	327.9386	327.9393	-2.16
	$C_{10}H_9BrN_3O^+$	265.9924	265.9931	-2.65
	$C_{10}H_7N_3O_3S^{+\cdot}$	249.0203	249.0210	-3.13
	$C_{10}H_7N_3O^{+\cdot}$	185.0584	185.0578	3.23
	$C_3H_{10}N^+$	60.0808	60.0809	-1.46
DP7(16.77)	$C_{12}H_{12}BrClN_3O^+$	327.9847	327.9851	-1.3
	$C_{12}H_{11}BrN_3O^+$	292.0080	292.0091	-3.63
	$C_{10}H_9BrN_3O^+$	265.9924	265.9924	0.93
	$C_{12}H_{12}ClN_3O^{+\cdot}$	249.0663	249.0670	-2.58
	$C_9H_8BrN_2O^+$	238.9815	238.9816	-0.6
	$C_{10}H_9N_3O^{+\cdot}$	187.0740	187.0736	1.96
DP8(21.92)	$C_{15}H_{19}BrClN_4O_3S^+$	449.0044	449.0050	-1.17
	$C_{12}H_{10}BrClN_3O_3S^+$	389.9309	389.9310	-0.08
	$C_{12}H_{12}BrClN_3O^+$	327.9847	327.9846	0.36
	$C_{12}H_{10}ClN_3O_3S^{+\cdot}$	311.0126	311.0128	-0.8
	$C_{12}H_{11}BrN_3O^+$	292.0080	292.0077	0.91
	$C_3H_{10}N^+$	60.0808	60.0806	3.31
DP9(23.82)	$C_{16}H_{14}Br_2N_5O_2^+$	465.9509	465.9516	-1.86
	$C_{12}H_{11}BrN_3O^+$	292.0080	292.0080	-0.44
	$C_4H_4BrN_2O^+$	174.9502	174.9507	-2.96
	$C_4H_2BrN_2^+$	156.9396	156.9393	1.54
DP10(19.98)	$C_{15}H_{20}BrN_4O_4S^+$	431.0383	431.0380	0.69
	$C_{13}H_{16}BrN_4O_3S^+$	387.0121	387.0120	0.38
	$C_{12}H_{11}BrN_3O_4S^+$	371.9648	371.9639	2.52
	$C_{10}H_7BrN_3O_3S^+$	327.9386	327.9381	1.5
	$C_{12}H_{11}N_3O_4S^{+\cdot}$	293.0465	293.0453	4.08
	$C_{10}H_9BrN_3O^+$	265.9924	265.9919	1.64
	$C_{10}H_7N_3O_3S^{+\cdot}$	249.0208	249.0199	1.52
	$C_{10}H_7N_3O^{+\cdot}$	185.0584	185.0592	-4.56
	$C_3H_{10}N^+$	60.0808	60.0806	2.74

Accepted Article

This article is protected by copyright. All rights reserved.

Figure 1.

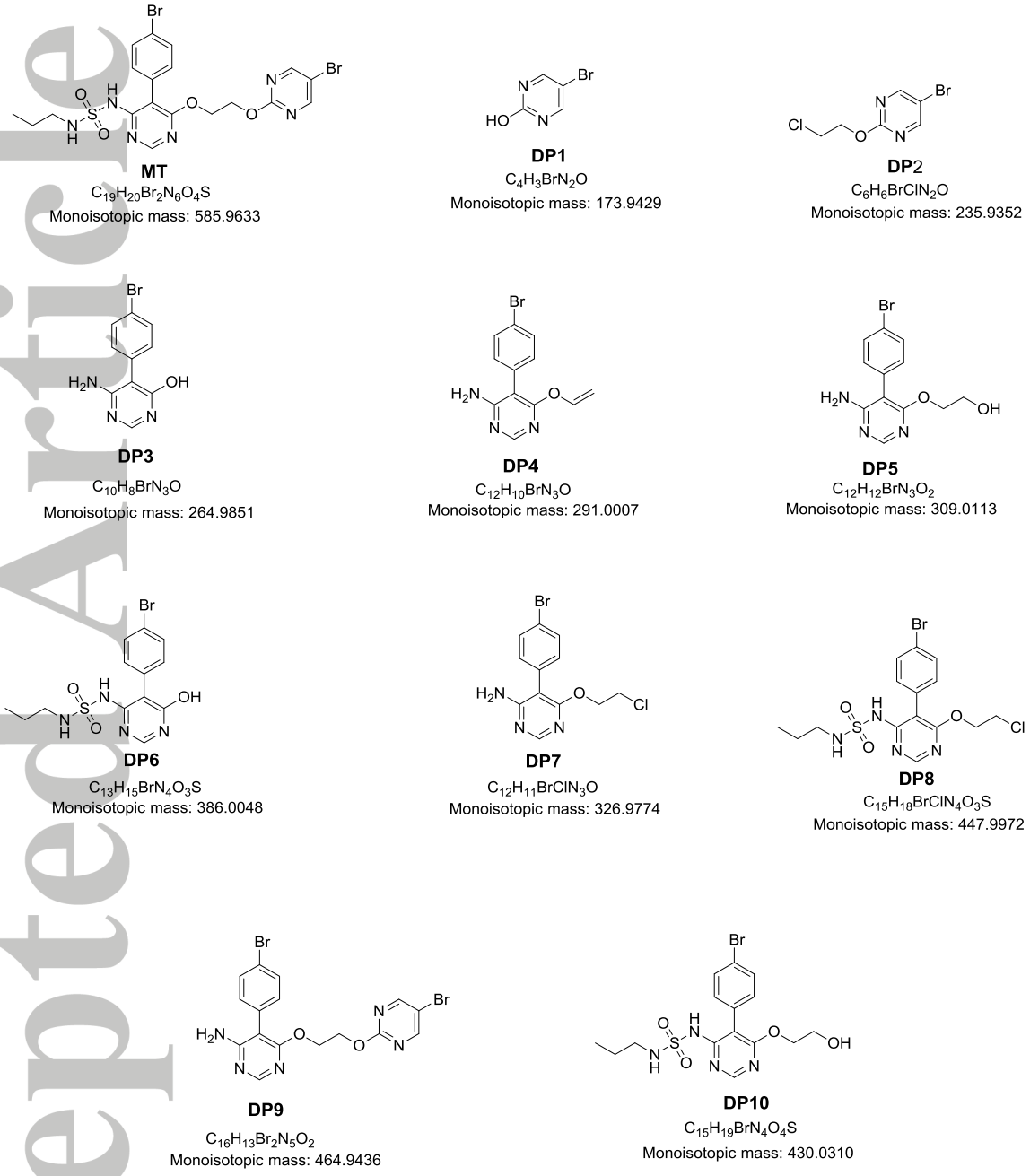

Figure 1. Chemical structures of MT and its degradation products.

Accepted Article

This article is protected by copyright. All rights reserved.

Scheme 1.

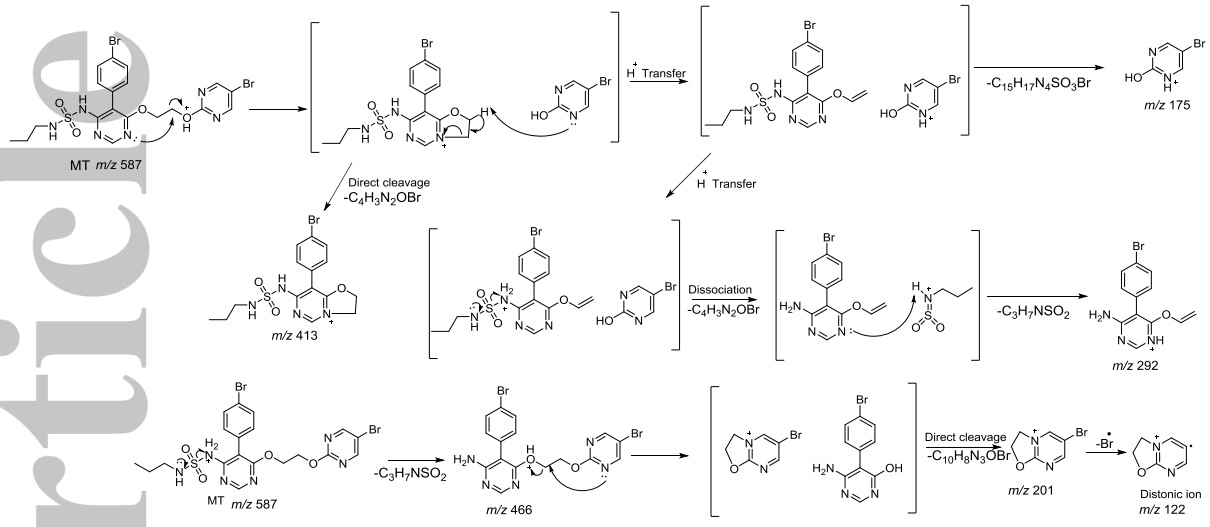

Scheme 1. Proposed fragmentation pathway for protonated MT.

Accepted Article

This article is protected by copyright. All rights reserved.

Scheme 2.

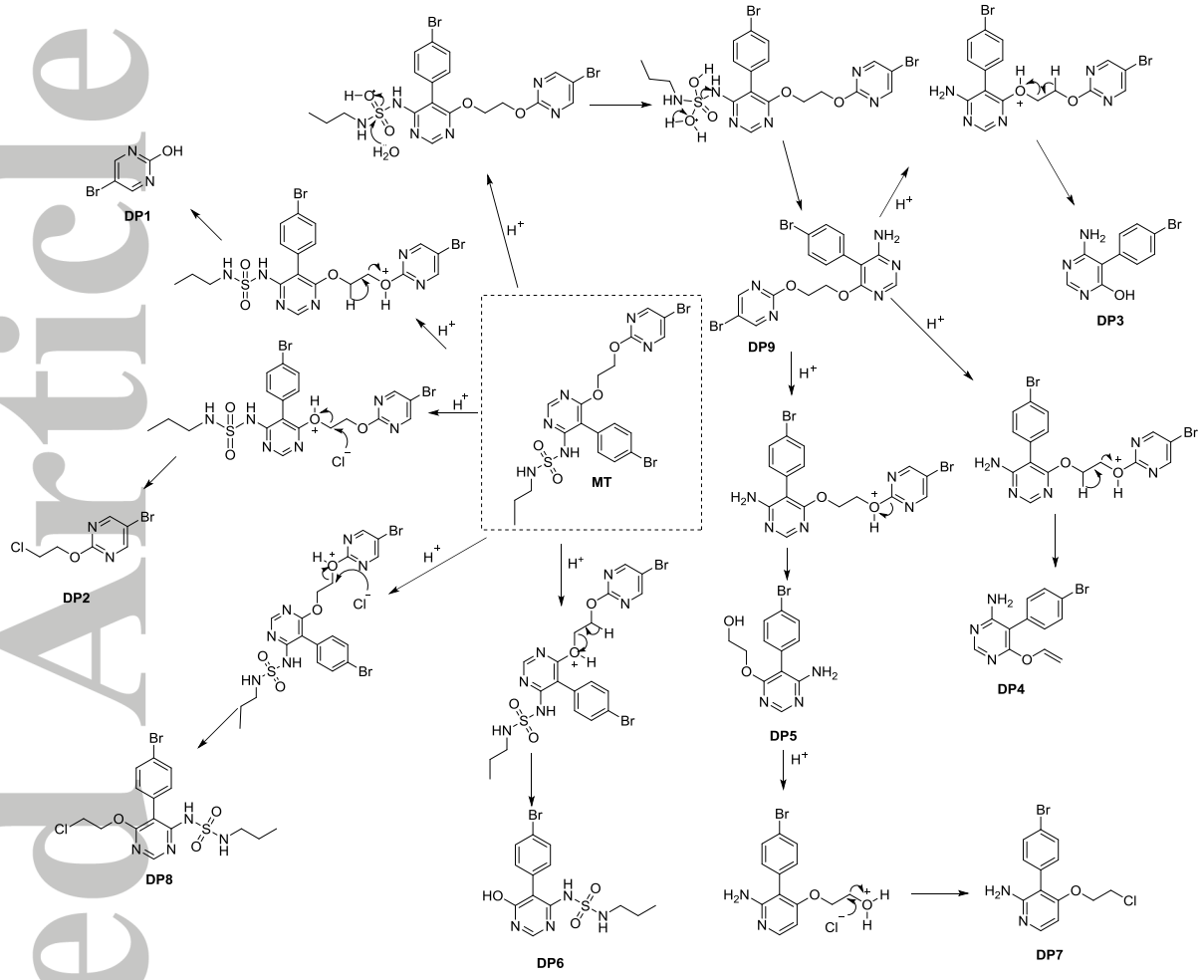

Scheme 2. Probable mechanism for the formation of DP1-DP9 under acidic hydrolytic condition.

Accepted Article

This article is protected by copyright. All rights reserved.

Scheme 3.

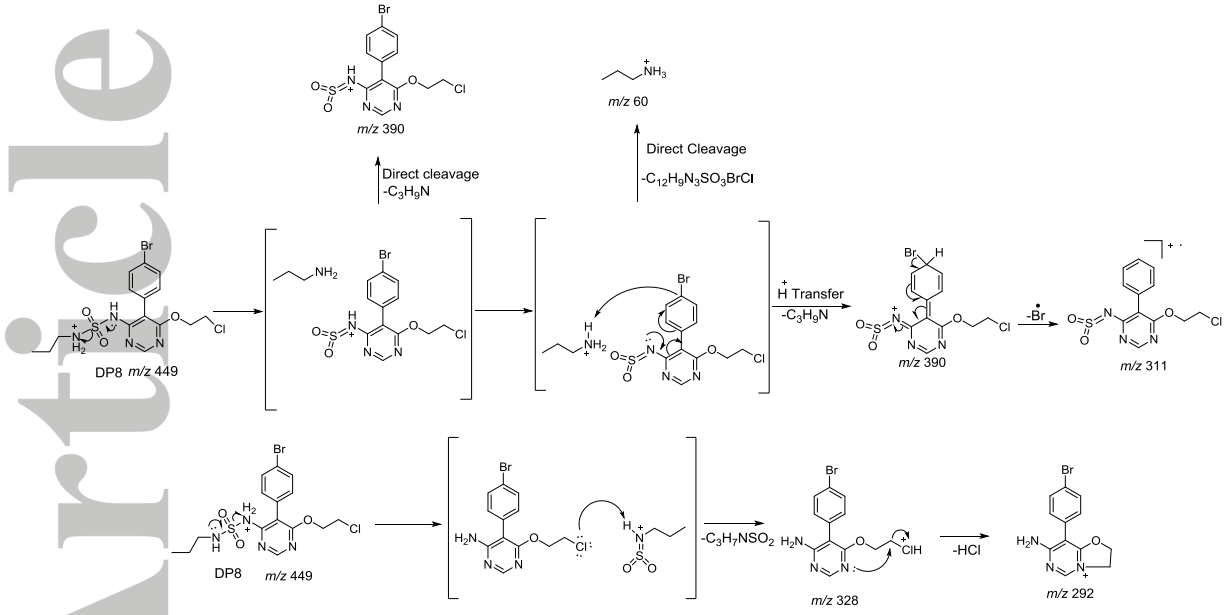

Scheme 3. Proposed fragmentation pathway for protonated DP8.

Accepted Article

This article is protected by copyright. All rights reserved.

Scheme 4.

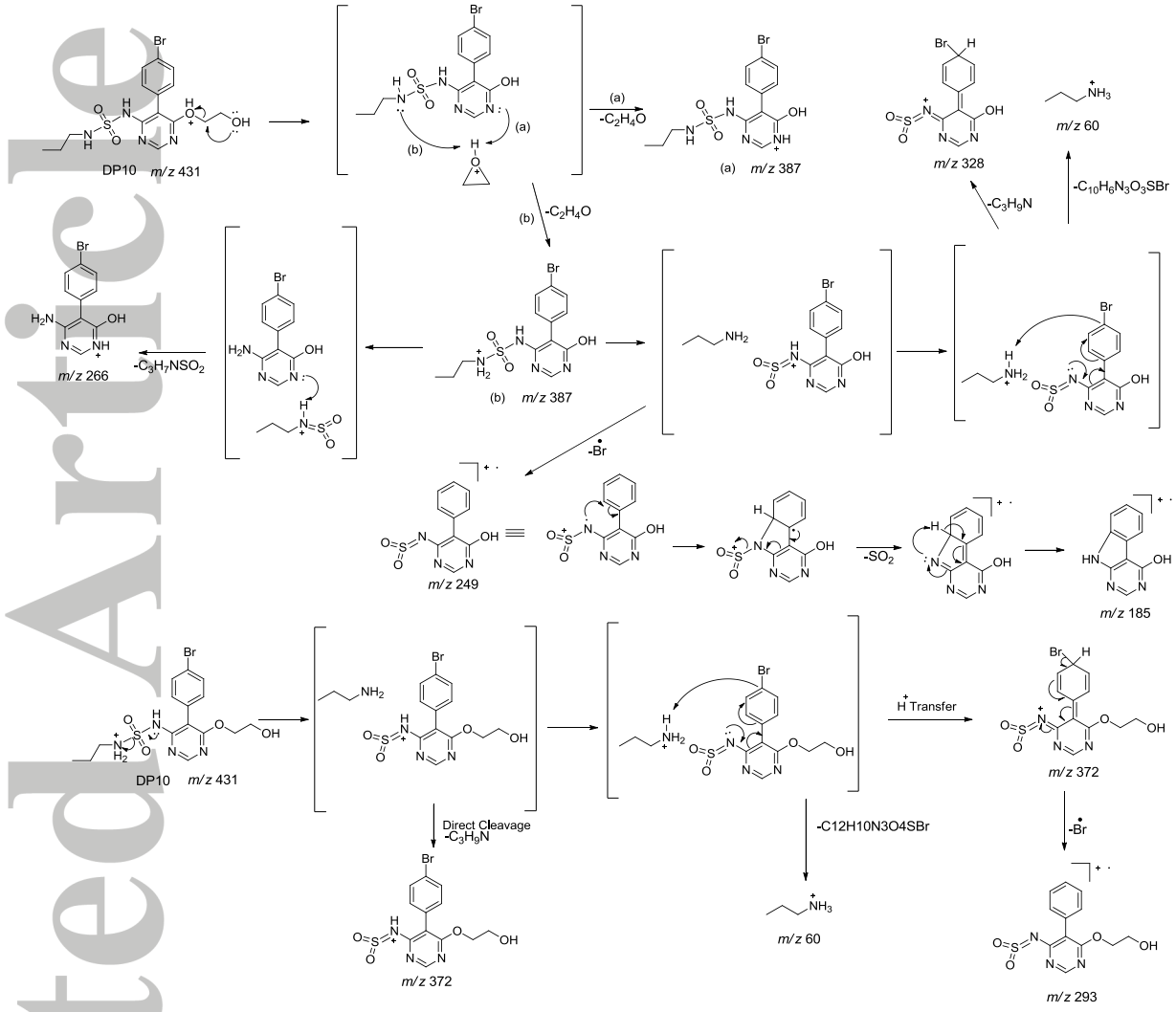

Scheme 4. Proposed fragmentation pathway for protonated DP10.

Accepted Article

This article is protected by copyright. All rights reserved.